



HAL
open science

High Resolution IMS-MS to Assign Additional Disulfide Bridge Pairing in Complementarity-Determining Regions of an IgG4 Monoclonal Antibody

Evolène Deslignière, Thomas Botzanowski, Hélène Diemer, Dale A Cooper-Shepherd, Elsa Wagner-Rousset, Olivier Colas, Guillaume Béchade, Kevin Giles, Oscar Hernandez-Alba, Alain Beck, et al.

► To cite this version:

Evolène Deslignière, Thomas Botzanowski, Hélène Diemer, Dale A Cooper-Shepherd, Elsa Wagner-Rousset, et al.. High Resolution IMS-MS to Assign Additional Disulfide Bridge Pairing in Complementarity-Determining Regions of an IgG4 Monoclonal Antibody. *Journal of The American Society for Mass Spectrometry*, 2021, 10.1021/jasms.1c00151 . hal-03287360v2

HAL Id: hal-03287360

<https://hal.science/hal-03287360v2>

Submitted on 27 Aug 2021

HAL is a multi-disciplinary open access archive for the deposit and dissemination of scientific research documents, whether they are published or not. The documents may come from teaching and research institutions in France or abroad, or from public or private research centers.

L'archive ouverte pluridisciplinaire **HAL**, est destinée au dépôt et à la diffusion de documents scientifiques de niveau recherche, publiés ou non, émanant des établissements d'enseignement et de recherche français ou étrangers, des laboratoires publics ou privés.



Distributed under a Creative Commons Attribution - NonCommercial - NoDerivatives 4.0 International License

High-Resolution IMS–MS to Assign Additional Disulfide Bridge Pairing in Complementarity-Determining Regions of an IgG4 Monoclonal Antibody

Evolène Deslignière,[§] Thomas Botzanowski,[§] H el ene Diemer, Dale A. Cooper-Shepherd, Elsa Wagner-Rousset, Olivier Colas, Guillaume B echade, Kevin Giles, Oscar Hernandez-Alba, Alain Beck, and Sarah Cianf erani*



Cite This: <https://doi.org/10.1021/jasms.1c00151>



Read Online

ACCESS |



Metrics & More

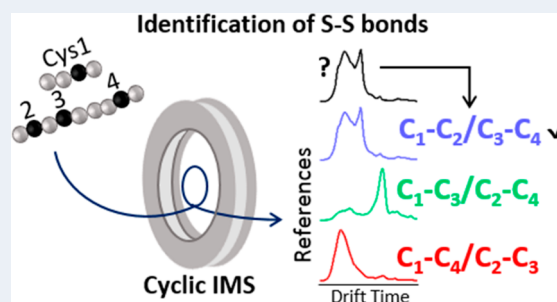


Article Recommendations



Supporting Information

ABSTRACT: Monoclonal antibodies (mAbs) have taken on an increasing importance for the treatment of various diseases, including cancers and immunological disorders. Disulfide bonds play a pivotal role in therapeutic antibody structure and activity relationships. Disulfide connectivity and cysteine-related variants are considered as critical quality attributes that must be monitored during mAb manufacturing and storage, as non-native disulfide bridges and aggregates might be responsible for loss of biological function and immunogenicity. The presence of cysteine residues in the complementarity-determining regions (CDRs) is rare in human antibodies but may be critical for the antigen-binding or deleterious for therapeutic antibody development. Consequently, in-depth characterization of their disulfide network is a prerequisite for mAb developability assessment. Mass spectrometry (MS) techniques represent powerful tools for accurate identification of disulfide connectivity. We report here on the MS-based characterization of an IgG4 comprising two additional cysteine residues in the CDR of its light chain. Classical bottom-up approaches after trypsin digestion first allowed identification of a dipeptide containing two disulfide bridges. To further investigate the conformational heterogeneity of the disulfide-bridged dipeptide, we performed ion mobility spectrometry–mass spectrometry (IMS–MS) experiments. Our results highlight benefits of high resolution IMS–MS to tackle the conformational landscape of disulfide peptides generated after trypsin digestion of a humanized IgG4 mAb under development. By comparing arrival time distributions of the mAb-collected and synthetic peptides, cyclic IMS afforded unambiguous assessment of disulfide bonds. In addition to classical peptide mapping, qualitative high-resolution IMS–MS can be of great interest to identify disulfide bonds within therapeutic mAbs.



INTRODUCTION

Monoclonal antibodies (mAbs) are 150 kDa tetrameric glycoproteins that have expanded the treatment of various diseases (cancer, arthritis, asthma, and diabetes).¹ Post-translational modifications (PTMs) such as deamidations, disulfide bridges, or glycosylation play crucial roles in mAb structure and activity. Among them, inter- and intrachain disulfide connectivity ensures proper mAb folding and stabilizes their native high-order conformations and consequently their biological function.^{2–4} Disulfide bonds can also lead to structural isoforms.⁵ mAbs are highly disulfide-bridged molecules constituted of two light (LC) and two heavy chains (HC), linked by 16 disulfide bonds for IgG1 and IgG4, 18 for IgG2, and 25 for IgG3. The LC is connected to the HC by one disulfide bond. HCs are linked by two (for IgG1 and IgG4), four (for IgG2), and 11 (for IgG3) disulfide bridges located in a short hinge region. Each IgG contains 12 intrachain bonds located in six different domains: one variable (VL) and one constant (CL) for the LCs and one variable (VH) and three

constant (CH1, CH2, CH3) for the HCs. Each variable domain mediates antigen recognition via three hypervariable loops called complementarity-determining regions (CDR), which interact with antigens and govern the specificity and potency of the mAb. Conversely to sharks and camels (scFv, VHH), the presence of cysteine residues in the CDRs is rare in human antibodies.^{6,7} However, some human antibodies have been reported to possess either one or two cysteine residues in the CDRs.^{7–9} To consider such antibodies with two Cys in the CDRs as potential drug candidate, full disulfide bridge pairing assessment is necessary.

Received: May 3, 2021

Revised: July 6, 2021

Accepted: July 7, 2021

As mAbs are highly disulfide-bonded therapeutics, it is crucial to ensure the correct assembly of disulfide connectivity and to evaluate the formation of mispaired disulfide linkages or chemical modifications to native disulfide bonds in the protein.¹⁰ For this, in-depth characterization of mAb-based products is required to ensure their safety and efficacy. Indeed, disulfide bridges represent important critical quality attributes (CQAs) that need to be closely monitored along the biotherapeutics' development to guarantee product quality, as scrambling or reduction of disulfide bonds can occur during manufacturing^{11,12} and storage.^{13,14} In particular, the presence of free cysteines, that is, in the reduced forms, may induce protein aggregation or non-native disulfide pairings,^{15–17} resulting in a potential loss of potency or immunogenicity of the biotherapeutic. These cysteine residues can be of concern when located in the CDRs of the antibody¹⁸ since their solvent exposure makes them more inclined to undergo PTMs.⁶ As an example, single unpaired cysteine in the CDR3 of the LC has been reported as cysteinylated or modified by oxidation,¹⁹ leading to complete inactivation of the antibody when both LCs were cysteinylated. As a result, IgGs with additional noncanonical cysteine are considered at risk during early developability assessment.

Assigning disulfide bridges is challenging as possible disulfide-bonded isomers increase significantly with the number of Cys residues. Hence, there is an increasing demand for efficient analytical methods for accurate characterization of disulfide bonds along the development process in order to (i) confirm the correct disulfide connectivity and (ii) verify the presence/absence of disulfide bond variants (non-native disulfide bonds). In this context, mass spectrometry (MS)-based techniques, and particularly liquid chromatography coupled to mass spectrometry (LC–MS) and tandem mass spectrometry (LC–MS/MS) methods, have self-settled as most attractive to tackle disulfide bond assessment.²⁰ However, MS characterization of disulfide bridges is not trivial and great care should be exercised to prevent disulfide bond scrambling during sample preparation and/or fragmentation in the mass spectrometer.²⁰ Bottom-up approaches based on enzymatic digestion followed by collision induced dissociation (CID) lead to the cleavage of the peptide backbone amide bonds but maintain the disulfide bond intact, hence producing diagnostic b and y ions comprising the disulfide bond, as well as ions that do not contain the disulfide bond. Electron transfer dissociation (ETD), which generates c and z ions, is also widely used for PTMs localization. However, ETD is not well adapted for disulfide connectivity assessment as cleavage of the disulfide bond is preferred (most intense ions in the MS/MS spectrum) over backbone fragmentation (minor c/z peaks that may contain or not the intact disulfide bond). Combination of both fragmentation techniques using MS³ look appealing and more successful, but are time-consuming.^{21,22} Both CID and ETD methods lead to poorly fragmented precursors for peptides with at least two intramolecular disulfide bonds, requiring further time-consuming manual MS/MS assignment.

However, all fragmentation techniques lack the information on low abundant disulfide variants/positional isomers. Ion mobility spectrometry coupled to mass spectrometry (IMS–MS), which separates ions based on their charge, shape and size in the gas phase, has been described in few papers as a promising approach to tackle disulfide-variant heterogeneity. IMS has proved valuable for the characterization of therapeutic mAbs, allowing to differentiate several isoforms of intact

antibodies²³ and to monitor batch-to-batch heterogeneity of disulfide pairings in antigens.²⁴ IMS has also been employed to determine topologies of disulfide-constrained isomeric peptides.²⁵ The group of De Pauw conducted several studies to investigate peptides bearing disulfide bridges, either by integrating IMS into CID and ETD workflows,^{26,27} or by using standalone IMS–MS.^{28,29} They first highlighted the structuring effect of disulfide bonds by comparing collision cross section (CCS) values of peptides bearing one to three intramolecular disulfide bridges with reduced reference peptides.²⁸ They demonstrated that classical traveling wave ion mobility spectrometry (TWIMS) can partially separate isomers bearing two intramolecular disulfide bonds. Molecular modeling can help to predict structural constraints related to different disulfide variants, which allows to infer theoretical CCS values and estimate the arrival time order.²⁹ However, structures with very close CCS, including highly constrained disulfide isomers for which Coulombic repulsion is prevented, lead to ambiguous disulfide pairing assignments due to insufficient resolution, the latter being limited by the length of linear TWIMS cells.^{28,29} Advancements in high resolution IMS offer new opportunities to tackle isomeric peptides, as exemplified by the clear separation of lasso peptides and their branched-cyclic analogs obtained on a trapped IMS (TIMS) instrument with a resolving power $R \sim 90\text{--}250 \Omega/\Delta\Omega$.^{30,31} Another study using high-resolution TIMS showed that the differentiation of disulfide-bridged peptide isomers was possible based on their individual IMS profiles, however determining the isomer composition of a mixture remains challenging without reference to a profile library, as each isomer may produce several features at once.³² Recently, Giles et al.³³ introduced a TWIMS-based high-resolution multipass cyclic ion mobility spectrometry (cIMS) instrument with increased path length allowing selectable resolving power. With the cIMS, $R \sim 750 \Omega/\Delta\Omega$ has been obtained after 100 passes for two isomeric pentapeptides. This type of cIMS device was shown to maintain native gas-phase structures of common proteins, including cytochrome *c* and concanavalin A.³⁴ Sisley et al.³⁵ illustrated the benefits of high-resolution cIMS to increase the number of detected proteins from mouse and rat tissues via liquid extraction surface analysis. Multipass high-resolution cIMS appears as an attractive technique to circumvent limitations of classical TWIMS cells for the elucidation of disulfide networks in peptides and proteins.

In this context, we report here on the disulfide identification of an IgG4 antibody containing two additional cysteine residues in the CDR of the LC at positions 91 and 100 (Figure S1). Peptide mapping first identified that the two additional Cys form two disulfide bridges. In order to assign correct disulfide bridge pairing, we performed IMS–MS on two platforms, a classical linear TWIMS platform and a higher resolution cyclic TWIMS instrument. We demonstrate the benefits of high-resolution cIMS–MS for the identification of two supplementary disulfide bonds in a humanized IgG4 mAb that contains two putative additional cysteines in the CDR3 of its LC. Finally, we highlight the advantages of multipass cIMS–MS for a better separation of conformers, with newly resolved species.

■ MATERIALS AND METHODS

Antibody and peptides production and purification.

The recombinant antibody was expressed in transiently transfected HEK293 cells at the Centre d'Immunologie Pierre

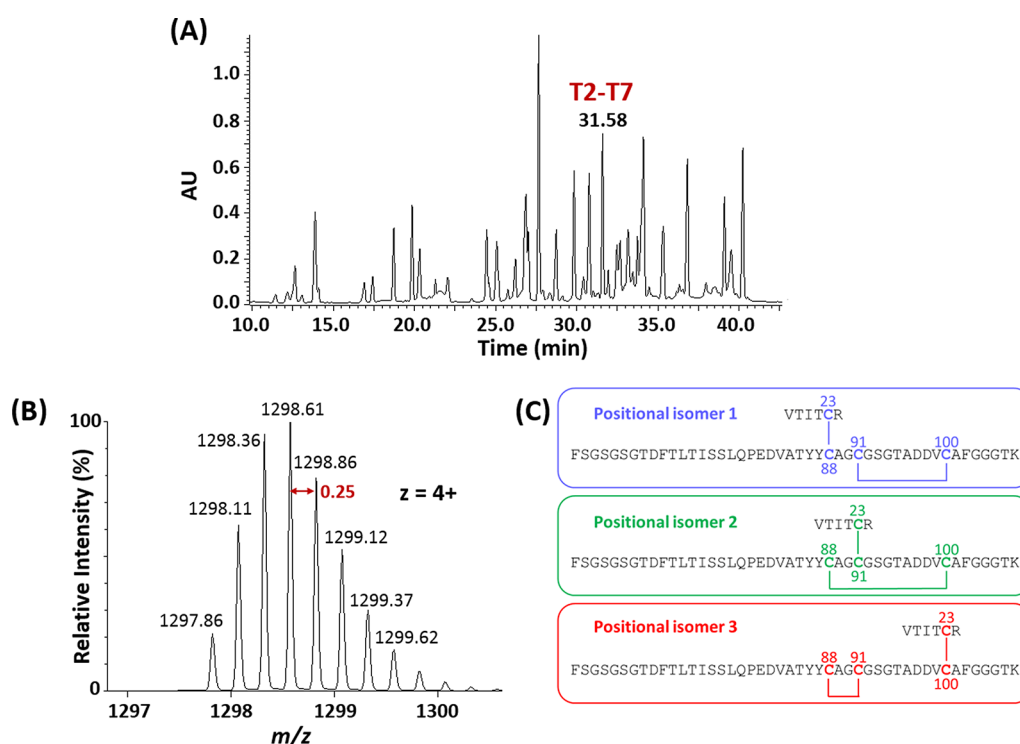


Figure 1. Bottom-up LC–MS experiments. LC–MS of the mAb tryptic digest was first carried out under nonreducing conditions, illustrated by (A) a UV chromatogram with an identified T2-T7 peak and (B) a MS spectrum zoomed on the 4+ charge state of T2-T7, indicating the presence of two disulfide bonds. (C) Representation of the three possible disulfide-bridged positional isomers of the T2-T7 peptide.

Fabre (Saint-Julien-en-Genevois, France) and purified using standard manufacturing procedures, including a protein A affinity chromatography step lead selection.²⁴ The synthetic peptides were produced and purified by standard manufacturing procedure.³⁶

Trypsin digestion. 100 μg of mAb were solubilized in 120 μL Tris Base 50 mM, CaCl_2 1 mM, 0.1% RapiGest (Waters, Wilmslow, UK), pH 7.1. Sample was incubated for 15 min at 80 $^\circ\text{C}$ under agitation (750 rpm). Fifteen μL of acetonitrile (ACN) were added, before digestion with 5 μL of 1 $\mu\text{g}/\mu\text{L}$ trypsin solution (i.e., enzyme/substrate ratio 1:20 (w:w)) for 3h30 at 37 $^\circ\text{C}$ under agitation (750 rpm). The sample was split in two aliquots of equal volume. One aliquot was reduced by adding 2.5 μL DTT 500 mM. The reduction was performed at 56 $^\circ\text{C}$ for 45 min under agitation (750 rpm). The reaction was stopped in both samples by adding 1 μL of trifluoroacetic acid (TFA). RapiGest was eliminated by heating at 37 $^\circ\text{C}$ for 30 min and by centrifugation at 10 000 g for 5 min.

LC–MS/MS. Samples were analyzed on an ACQUITY UPLC H-Class system (Waters, Wilmslow, UK) coupled to a Synapt G2-Si quadrupole/TWIMS/time-of-flight (Q-TWIMS-ToF) mass spectrometer (Waters). The system was fully controlled by MassLynx v4.1. 50 pmol of sample preparation were injected on an ACQUITY UPLC BEH C18 column, 130 \AA , 1.7 μm , 2.1 \times 300 mm (Waters) set at 80 $^\circ\text{C}$. The gradient was generated at a flow rate of 250 $\mu\text{L}/\text{min}$ using 0.1% TFA for mobile phase A and ACN containing 0.08% TFA for mobile phase B. Mobile phase B was raised from 5 to 43% in 38 min and to 80% in 2 min. For synthetic peptides, mobile phase B was raised from 25 to 40% in 15 min. Eluted samples from the column were detected by UV at 214 and 254 nm, and by MS. The Synapt G2-Si was operated in positive ionization mode with a capillary voltage of 3 kV and a sample cone

voltage of 40 V. For tandem MS experiments performed in data-dependent acquisition mode, the system was operated with automatic switching between MS (1 s/scan on m/z range [300;1800]) and MS/MS modes (1 s/scan on m/z range [50;2000]). The two most abundant peptides were selected on each MS spectrum for further isolation, and CID fragmentation using a collision energy ramp with the following settings: low mass (200 m/z) collision energy ramp from 6 to 20 eV, high mass (2000 m/z) collision energy ramp from 45 to 100 eV. Fragmentation was performed using argon as the collision gas. Glu-FibrinoPeptide was used for the ToF calibration and as lock-mass correction.

The T2-T7 peptide was manually collected in a time window of 30 s, corresponding to a fraction of ~ 125 μL . CID experiments on the collected and synthetic peptides were carried out by direct infusion on the same mass spectrometer at a collision energy of 38 eV. The fragmentation spectra were deconvoluted with MaxEnt3 algorithm (Waters) and manually interpreted.

IMS–MS experiments on Synapt G2 HDMS. Samples were diluted to 10 μM with a 50/49/1 (v/v/v) water/ACN/formic acid solution before IMS–MS experiments. IMS–MS measurements were performed using a Synapt G2 Q-TWIMS-ToF instrument (Waters, Wilmslow, UK) coupled to an automated chip-based nanoESI device (TriVersa NanoMate, Advion, Ithaca, USA). The Synapt G2 was operated in positive ionization mode. The cone voltage of the source interface was fixed to 40 V. The TWIMS wave height and velocity were adjusted to 40 V and 1200 m/s, respectively. The cooling (He) and IMS separation (N_2) gas flow rates were set to 150 and 50 mL/min, respectively, giving a pressure of 3.3 mbar in the linear TWIMS cell. The IMS resolving power of this instrument is $\sim 40 \Omega/\Delta\Omega$.

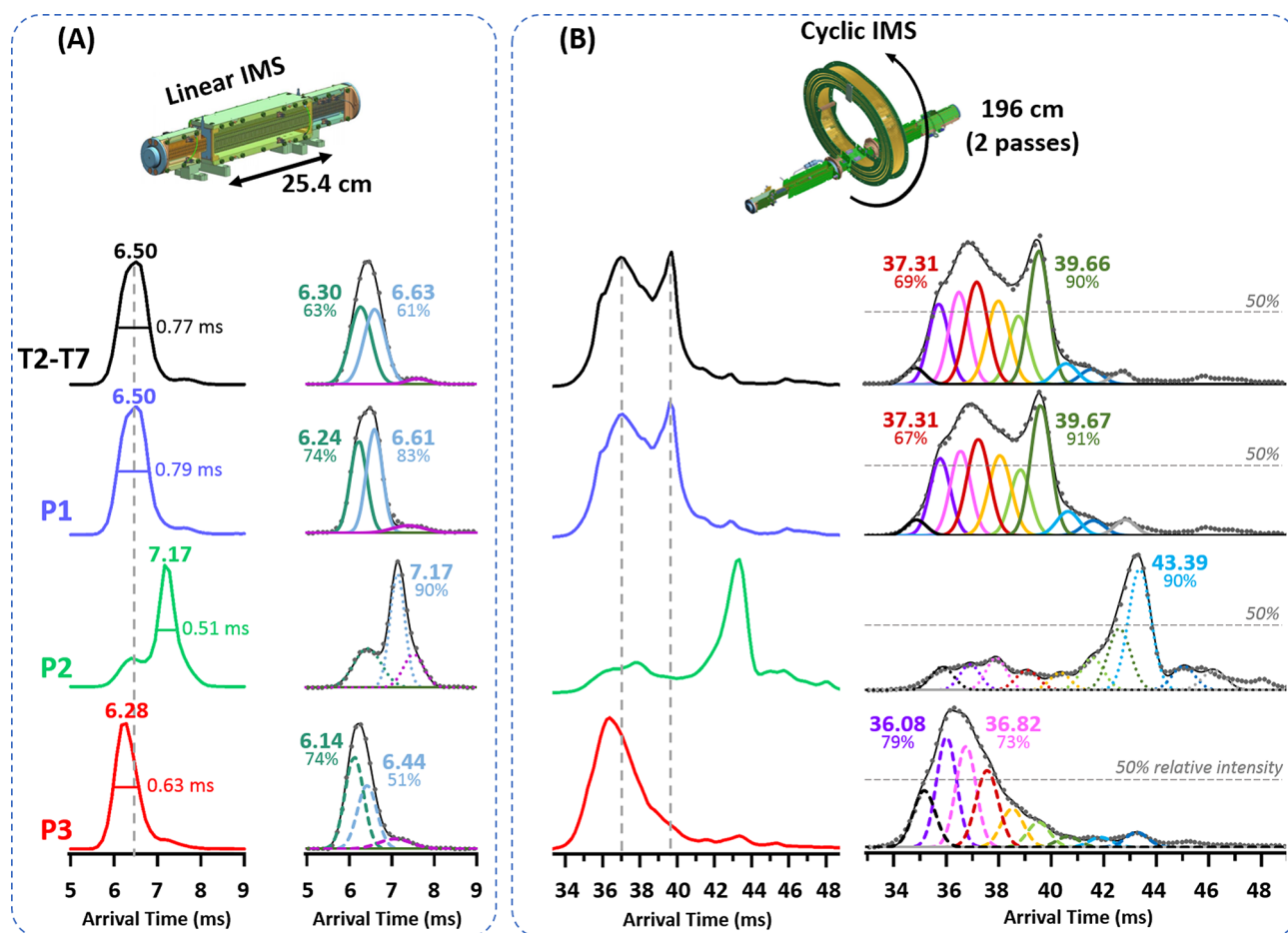


Figure 2. IMS–MS experiments performed on two different IMS instruments. ATDs were obtained for the 4+ charge state of the collected T2–T7 peptide (black), and the three synthetic peptides corresponding to disulfide-bridged variants P1 (blue), P2 (green), and P3 (red). (A) Results obtained on a linear TWIMS instrument. Extracted ATDs (left) were further investigated using Gaussian fitting (right), highlighting the existence of multiple conformers. Gray dots correspond to experimental data, while thin black lines represent combined fits. (B) Extracted ATDs (left) obtained on a cIMS platform after two passes, and their corresponding Gaussian fits (right).

IMS–MS experiments on cIMS. Samples were analyzed under the same solution conditions as the SYNAPT G2. Cyclic IMS–MS measurements were performed on a SELECT SERIES Cyclic IMS instrument³³ (Waters, Wilmslow, UK) which has a Q-cyclicTWIMS-ToF geometry. Peptide solutions were electrosprayed in positive ionization mode from PicoTipTM GlassTipTM borosilicate glass nanoflow capillaries (NewObjective, Woburn, MA, USA). The cone voltage was set at 40 V. The TWIMS wave height was set at 22 V with a velocity of 375 m/s. The helium cell and IMS separation gas flow rates were 150 and 45 mL/min, respectively, giving rise to a cIMS cell pressure of 1.7 mbar. Data were acquired with either one or two passes of the cyclic device. For higher mobility resolving power, ions corresponding to the front or rear portions of the arrival time distributions after one pass were selectively retained in the cyclic device for an additional four passes (for a total of five passes) by tuning the timings and voltages of the multifunctional ion entry/exit array.³³ All data were acquired on the quadrupole-isolated 4+ charge states of the fractionated and synthetic peptides (m/z 1298).

IMS–MS data treatment and Gaussian fitting. IMS–MS data were analyzed using MassLynx v4.1. Arrival time distributions (ATDs) were extracted in the m/z range [1297;1301]. Gaussians were fitted to the extracted ATDs using the “Gaussian Fitting” module of the CIUSuite 2

software.³⁷ Gaussian fitting was performed in the protein only mode, with all signals considered to be related to the analyte. The following parameters were used for all ATDs: minimum peak amplitude = 0.05; maximum protein components fitted = 10; peak overlap penalty mode = relaxed, which penalizes overlaps > ~ 85%, but allows overlapping peaks to be chosen if other solutions are poorly fitted. In order to “calibrate” the Gaussian fitting process, the expected fwhm of fits was determined using slicing experiments performed on a synthetic peptide³³ (Figure S2A). Briefly, one population was selected and ejected to the prestore while other populations were ejected to the ToF. This allows to have a better definition of the selected slice upon reinjection into the cIMS cell, providing an accurate fwhm measurement of the main feature contained within the slice (Figure S2A, B). After one pass, the major feature of our isolated slice exhibits a fwhm of 0.65 ms. In multipass mode, the expected fwhm of a peak containing a single conformer should scale with the square root of the number of passes.³³ At two passes, the measured fwhm (0.94 ms) matches well with the theoretical value (0.92 ms), meaning that the selected feature does correspond to a unique conformer. These fwhm values were subsequently used as references to fit single species: fwhm(1 pass) = 0.65 ms, fwhm(2 passes) = 0.92 ms, fwhm(4 passes) = 1.45 ms. Peak

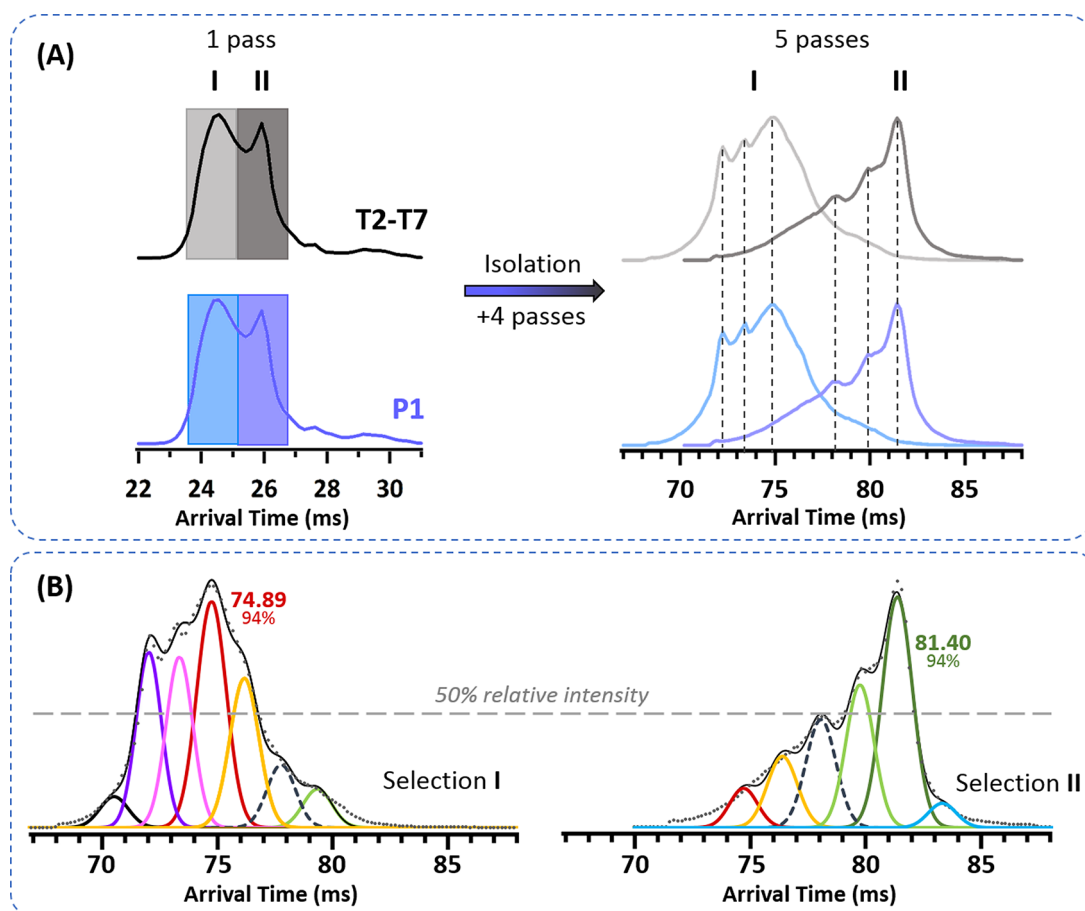


Figure 3. cIMS isolation experiments. (A) After one pass, the main features of T2-T7 (gray boxes) and P1 (blue boxes) were sequentially isolated in the cIMS device and subjected to four additional passes. ATDs of isolated features were extracted after a total of five passes. (B) Gaussian fitting of the two T2-T7 selected windows after five passes. Gray dots correspond to experimental data, while thin black lines represent combined fits. When already identified after two passes (Figure 2B), the same color code as in Figure 2B is used. One additional conformer is detected after five passes, represented with a dashed line (dark gray).

width tolerance was set to ± 0.05 ms. Combined fits were in good agreement with experimental data ($r^2 > 0.99$).

RESULTS

Peptide mapping and identification of disulfide-containing peptides. Classical MS strategies rely on indirect proof of disulfide bridge existence by comparing reduced and nonreduced samples. We thus first performed peptide mapping after trypsin digestion, one of the common techniques used for disulfide bridge pairing assessment (Figure 1). Differential analysis of peptide maps obtained under reducing and nonreducing conditions allowed identification of a dipeptide of the CDR3 (Figure S1) of the LC (peptide T2-T7, Figure 1A) bearing two additional disulfide bonds (experimental monoisotopic mass 5187.41 Da) in agreement with the presence of four cysteine residues (Cys91/100/23/88). Careful investigation of the isotopic distribution of the 3+ and 4+ charge states of T2-T7 peptide allowed to rule out the presence of species with only one disulfide bridge, whose isotopic distribution would overlap with the dipeptide containing 2 S–S bridges (Figure 1B and S3). Three possible isomeric disulfide variants can be expected from the amino acid sequence of T2-T7 (Figure 1C).

IMS–MS analysis to establish T2-T7 disulfide pairings conformational heterogeneity. Instead of conventional

peptide mapping approaches, we intended to use IMS–MS, which has already proved to be a valuable and efficient tool to differentiate disulfide-bridged protein and peptide isomers,^{23,24,28,29,32} to identify T2-T7 disulfide bridge pairing. To this aim, the T2-T7 fraction was manually collected, and its ATD compared to those obtained from synthetic peptide isomers (P1, P2 and P3) corresponding to the possible combinations of disulfide bonds (Figure 1C), on two IMS–MS platforms with different IMS resolutions.

IMS–MS experiments were first performed on the Synapt linear TWIMS instrument (Figure 2A). The 4+ charge state of T2-T7 exhibits a broad IMS ATD centered on ~ 6.50 ms. While a bimodal distribution is observed for P2, both P1 and P3 present primarily broad ATD features, centered on ~ 6.50 and 6.28 ms, respectively. As broad ATDs might suggest coexistence of multiple conformers, we then used Gaussian fitting (see Materials and Methods) as indication of multiple populations present for each peptide. For T2-T7, P1, and P3, Gaussian detection allows the identification of two main populations along with a minor one of lower mobility (relative intensity $< 10\%$). Overall, based on arrival time and ATD profile, these IMS–MS results might suggest that T2-T7 is similar to P1, even if P3 cannot be definitively ruled out (different peak shapes but very close ATDs and same number of conformers). Of note, P1 and P3 were also found to coelute in reversed-phase liquid chromatography (rpLC), avoiding the

use of rpLC in front of IMS–MS to separate isomeric peptides (Figure S4).

As the different conformers were not resolved at the linear TWIMS resolving power of around $40 \Omega/\Delta\Omega$, we next performed IMS experiments on the quadrupole-isolated 4+ charge state of each peptide on the higher resolution cyclic IMS instrument (Figure 2B). As cIMS generates complex ATD profiles, we used Gaussian fitting as an indicative tool for conformer heterogeneity assessment from IMS patterns. As the deconvolution of ATDs strongly depends on fitting parameters, the number of detected features was used as an indication of the conformer heterogeneity to illustrate how high-resolution can improve the separation of conformers, and help to understand differences that appear between the various isomeric peptides. After one cIMS pass ($R \sim 65 \Omega/\Delta\Omega$), T2-T7 reveals a highly heterogeneous ATD, with at least five conformers (fwhm = 0.65 ms) previously overlapped within a broad ATD on the linear TWIMS platform (Figure S5). Although the benefits of cIMS–MS over linear TWIMS to detect multiple conformers are already clear after one pass, populations could potentially be better resolved with more passes. Indeed, after two cIMS passes ($R \sim 92 \Omega/\Delta\Omega$), new features are uncovered, highlighting the advantages of multipass cIMS–MS for improved conformational characterization (Figure 2B). Additional contributions to the main peaks could be detected based on our fitting parameters (fwhm = 0.92 ms), with six major species with relative intensities estimated >45%. Several minor conformers with lower relative intensities (<20%) were also fitted.

After two passes, ATDs of all synthetic peptides show additional features, unveiling broad conformational spaces (Figure 2B). T2-T7 and P1 present highly similar profiles with equivalent arrival times and relative intensities for all detected conformers. Overall, both peptides comprise two main contributions (>65%) centered on ~ 37.31 and 39.66 ms. Conversely, P2 and P3 exhibit only one major peak in their ATD profiles, and several minor populations. Fewer features are contained within the main peak of P2 and P3 (two and four conformers, respectively) compared to T2-T7/P1, in agreement with preliminary fwhm's obtained using linear TWIMS (Figure 2A), suggesting that T2-T7 possesses a higher degree of freedom for conformational changes.

As species of interest can be isolated based on their mobility in the cIMS device while the rest of the ions are ejected,³³ the two main peaks of T2-T7 peptides and P1 were further investigated. Ions in each mobility window, depicted I and II in Figure 3, were selectively isolated after one pass and subjected to four more passes, leading to a total of five passes ($R \sim 145 \Omega/\Delta\Omega$). Strictly identical isolated-profiles were obtained after five passes for the synthetic peptide P1, which strongly corroborates the assignment of disulfide bonds established after two passes (Figure 3A). The sequential isolation of windows I and II revealed that selection I comprises four main ion populations >50%, whereas selection II consists of two dominant features (Figure 3B). For both isolated windows, the detected conformers (fwhm = 1.45 ms) appear to be coherent with those obtained at two passes (same color code in Figure 2B and 3B), indicating that no activation toward more extended/compact species occurs within the time frame of the four additional passes. No interconversion between the two main conformers is observed.

Altogether, based on the sole use of IMS–MS data, these results allowed to unambiguously conclude that peptides T2-

T7 and P1 bear similar cysteine connectivities, with disulfide bonds corresponding to Cys23-Cys88 and Cys91-Cys100 in agreement with classical peptide mapping results (Figure S6). In addition, our results highlight the benefit of high resolution IMS instrumentation for more accurate qualitative identification of disulfide peptides compared to linear TWIMS, relying on peak shapes and arrival times. cIMS offers more definition of the ATDs with several newly resolved species apparent (including low abundant ones) compared to the lower resolution linear TWIMS. Multipass cIMS allowed a better separation of conformers, identification of low abundant ones and finally better assignment/identification of the disulfide connectivities.

CONCLUSIONS

We have presented here the potential of high-resolution IMS for rapid and unambiguous profiling of disulfide pairings in an IgG4 with two additional Cys residues in the CDR of its light chain. First, a classical bottom-up approach after tryptic digestion allowed identification of a peptide containing two disulfide bonds. A comparison between ATDs obtained on the cIMS device for the mAb-collected and synthetic peptides provided unequivocal determination of disulfide bridges. While linear TWIMS results were ambiguous, benefits of higher IMS resolutions obtained on a cyclic instrument were clearly illustrated. Indeed, the gas-phase conformational heterogeneity of this disulfide-bridged peptide investigated through cIMS–MS experiments revealed broader conformational landscapes than on a linear TWIMS. Our work illustrates the ability of high resolution IMS to solve tricky analytical issues related to the identification of disulfide conformers through high resolution separation of isomeric peptides.

Multipass high resolution cIMS helps to circumvent current analytical limitations related to the elucidation of cysteine connectivity and conformational heterogeneity. Indeed, the main bottleneck of classical bottom-up approaches used for disulfide bonds characterization remains the tedious treatment of MSⁿ data. ETD and CID both require extensive and manual data analysis, leading to highly time-consuming processes, especially if the protein is cysteine-rich. While IMS appears as an elegant technique to complement bottom-up strategies, the resolution inherent to linear TWIMS cells sometimes prevents the separation of disulfide-bridged isomers. Our study highlights the benefits of multipass high resolution cIMS to clearly differentiate isomeric disulfide-bonded peptides based solely on ATD profiles. By minimizing the need for laborious manual data analysis, the cyclic IMS approach described here thus has the potential to become a straightforward qualitative tool for accurate characterization of low abundant conformers in biological samples.

In particular, multipass cIMS could be of great interest for a rapid in-depth disulfide identification of a wide range of mAb-related products, as incorrectly folded forms need to be closely monitored during biotechnological development to ensure drug quality. We envision that multipass cIMS will help to decipher disulfide networks not only for peptides but also for large intact mAb formats comprising more complex cysteine connectivity.

ASSOCIATED CONTENT

Supporting Information

The Supporting Information is available free of charge at <https://pubs.acs.org/doi/10.1021/jasms.1c00151>.

Amino acid sequence corresponding to the light chain of mAb hzIgG4 (Figure S1); determination of the expected fwhm for a single conformation (Figure S2); theoretical and experimental isotopic distributions for the 4+ charge state of T2-T7 peptide (Figure S3); extracted ion chromatograms obtained in rpLC for the three synthetic peptides P1–P3 (Figure S4); cIMS–MS experiments after one pass (Figure S5); deconvoluted CID MS/MS fragment-ion spectrum obtained for the collected fraction of T2-T7 ($z = 4+$, m/z 1297.86), with deduced fragmentation sequence (Figure S6) (PDF)

AUTHOR INFORMATION

Corresponding Author

Sarah Cianféran – *Laboratoire de Spectrométrie de Masse BioOrganique (LSMBO), IPHC, UMR 7178, Université de Strasbourg, CNRS, 67087 Strasbourg, France; Infrastructure Nationale de Protéomique ProFI – FR2048, 67087 Strasbourg, France; orcid.org/0000-0003-4013-4129; Phone: +33 (0)3 68 85 26 79; Email: sarah.cianferani@unistra.fr; Fax: +33 (0)3 68 85 27 81*

Authors

Evolène Deslignière – *Laboratoire de Spectrométrie de Masse BioOrganique (LSMBO), IPHC, UMR 7178, Université de Strasbourg, CNRS, 67087 Strasbourg, France; Infrastructure Nationale de Protéomique ProFI – FR2048, 67087 Strasbourg, France*

Thomas Botzanowski – *Laboratoire de Spectrométrie de Masse BioOrganique (LSMBO), IPHC, UMR 7178, Université de Strasbourg, CNRS, 67087 Strasbourg, France; Infrastructure Nationale de Protéomique ProFI – FR2048, 67087 Strasbourg, France*

Hélène Diemer – *Laboratoire de Spectrométrie de Masse BioOrganique (LSMBO), IPHC, UMR 7178, Université de Strasbourg, CNRS, 67087 Strasbourg, France; Infrastructure Nationale de Protéomique ProFI – FR2048, 67087 Strasbourg, France*

Dale A. Cooper-Shepherd – *Waters Corporation, Cheshire SK9 4AX, U.K.*

Elsa Wagner-Rousset – *IRPF - Centre d'Immunologie Pierre-Fabre (CIPF), 74160 Saint-Julien-en-Genevois, France*

Olivier Colas – *IRPF - Centre d'Immunologie Pierre-Fabre (CIPF), 74160 Saint-Julien-en-Genevois, France*

Guillaume Béchade – *Waters Corporation, Cheshire SK9 4AX, U.K.*

Kevin Giles – *Waters Corporation, Cheshire SK9 4AX, U.K.; orcid.org/0000-0001-5693-1064*

Oscar Hernandez-Alba – *Laboratoire de Spectrométrie de Masse BioOrganique (LSMBO), IPHC, UMR 7178, Université de Strasbourg, CNRS, 67087 Strasbourg, France; Infrastructure Nationale de Protéomique ProFI – FR2048, 67087 Strasbourg, France*

Alain Beck – *IRPF - Centre d'Immunologie Pierre-Fabre (CIPF), 74160 Saint-Julien-en-Genevois, France; orcid.org/0000-0002-4725-1777*

Complete contact information is available at:
<https://pubs.acs.org/10.1021/jasms.1c00151>

Author Contributions

[§]E.D. and T.B. contributed equally to this part.

Funding

This work was supported by the CNRS, the University of Strasbourg, the “Agence Nationale de la Recherche”, and the French Proteomic Infrastructure (ProFI; ANR-10-INBS-08–03).

Notes

The authors declare no competing financial interest.

ACKNOWLEDGMENTS

We thank GIS IBI SA and Région Alsace for financial support in purchasing a Synapt G2 HDMS instrument. E.D. and T.B. acknowledge the French Ministry for Education and Research and the Institut de Recherches Servier, for funding of their Ph.D. works, respectively.

ABBREVIATIONS

ATD, arrival time distribution; CCS, collision cross section; CDR, complementarity-determining region; CH, heavy-chain constant domain; CID, collision-induced dissociation; cIMS, cyclic ion mobility spectrometry; CL, light-chain constant domain; CQA, critical quality attribute; ETD, electron-transfer dissociation; HC, heavy chain; LC, light chain; IMS–MS, ion mobility spectrometry–mass spectrometry; LC–MS, liquid chromatography coupled to mass spectrometry; LC–MS/MS, liquid chromatography coupled to tandem mass spectrometry; mAb, monoclonal antibody; MS, mass spectrometry; MS/MS, tandem mass spectrometry; PTM, post-translational modification; rpLC, reversed-phase liquid chromatography; TIMS, trapped ion mobility spectrometry; TWIMS, traveling wave ion mobility spectrometry; VH, heavy-chain variable domain; VL, light-chain variable domain

REFERENCES

- (1) Kaplon, H.; Reichert, J. M. Antibodies to watch in 2021. *mAbs* **2021**, *13* (1), 1860476.
- (2) Alewood, D.; Nielsen, K.; Alewood, P. F.; Craik, D. J.; Andrews, P.; Nerrie, M.; White, S.; Domagala, T.; Walker, F.; Rothacker, J.; Burgess, A. W.; Nice, E. C. The role of disulfide bonds in the structure and function of murine epidermal growth factor (mEGF). *Growth Factors* **2005**, *23* (2), 97–110.
- (3) Zhang, L.; Chou, C. P.; Moo-Young, M. Disulfide bond formation and its impact on the biological activity and stability of recombinant therapeutic proteins produced by *Escherichia coli* expression system. *Biotechnol. Adv.* **2011**, *29* (6), 923–929.
- (4) Góngora-Benítez, M.; Tulla-Puche, J.; Albericio, F. Multifaceted Roles of Disulfide Bonds. Peptides as Therapeutics. *Chem. Rev.* **2014**, *114* (2), 901–926.
- (5) Wypych, J.; Li, M.; Guo, A.; Zhang, Z.; Martinez, T.; Allen, M. J.; Fodor, S.; Kelner, D. N.; Flynn, G. C.; Liu, Y. D.; Bondarenko, P. V.; Ricci, M. S.; Dillon, T. M.; Balland, A. Human IgG2 Antibodies Display Disulfide-mediated Structural Isoforms. *J. Biol. Chem.* **2008**, *283* (23), 16194–16205.
- (6) Xu, Y.; Wang, D.; Mason, B.; Rossomando, T.; Li, N.; Liu, D.; Cheung, J. K.; Xu, W.; Raghava, S.; Katiyar, A.; Nowak, C.; Xiang, T.; Dong, D. D.; Sun, J.; Beck, A.; Liu, H. Structure, heterogeneity and developability assessment of therapeutic antibodies. *mAbs* **2019**, *11* (2), 239–264.
- (7) Almagro, J. C.; Raghunathan, G.; Beil, E.; Janecki, D. J.; Chen, Q.; Dinh, T.; LaCombe, A.; Connor, J.; Ware, M.; Kim, P. H.; Swanson, R. V.; Fransson, J. Characterization of a high-affinity human antibody with a disulfide bridge in the third complementarity-determining region of the heavy chain. *J. Mol. Recognit.* **2012**, *25* (3), 125–135.
- (8) Banks, D. D.; Gadgil, H. S.; Pipes, G. D.; Bondarenko, P. V.; Hobbs, V.; Scavozze, J. L.; Kim, J.; Jiang, X.-R.; Mukku, V.; Dillon, T.

- M. Removal of Cysteinylation from an Unpaired Sulfhydryl in the Variable Region of a Recombinant Monoclonal IgG1 Antibody Improves Homogeneity, Stability, and Biological Activity. *J. Pharm. Sci.* **2008**, *97* (2), 775–790.
- (9) Gadgil, H. S.; Bondarenko, P. V.; Pipes, G. D.; Dillon, T. M.; Banks, D.; Abel, J.; Kleemann, G. R.; Treuheit, M. J. Identification of cysteinylation of a free cysteine in the Fab region of a recombinant monoclonal IgG1 antibody using Lys-C limited proteolysis coupled with LC/MS analysis. *Anal. Biochem.* **2006**, *355* (2), 165–174.
- (10) Moritz, B.; Stracke, J. O. Assessment of disulfide and hinge modifications in monoclonal antibodies. *Electrophoresis* **2017**, *38* (6), 769–785.
- (11) Trexler-Schmidt, M.; Sargis, S.; Chiu, J.; Sze-Khoo, S.; Mun, M.; Kao, Y.-H.; Laird, M. W. Identification and prevention of antibody disulfide bond reduction during cell culture manufacturing. *Biotechnol. Bioeng.* **2010**.
- (12) Hutterer, K. M.; Hong, R. W.; Lull, J.; Zhao, X.; Wang, T.; Pei, R.; Le, M. E.; Borisov, O.; Piper, R.; Liu, Y. D.; Petty, K.; Apostol, I.; Flynn, G. C. Monoclonal antibody disulfide reduction during manufacturing. *mAbs* **2013**, *5* (4), 608–613.
- (13) Yoshioka, S.; Aso, Y.; Izutsu, K. i.; Terao, T. Aggregates Formed During Storage of Beta-Galactosidase in Solution and in the Freeze-Dried State. *Pharm. Res.* **1993**, *10* (5), 687–691.
- (14) Chandrasekhar, S.; Topp, E. M. Thiol–Disulfide Exchange in Peptides Derived from Human Growth Hormone During Lyophilization and Storage in the Solid State. *J. Pharm. Sci.* **2015**, *104* (4), 1291–1302.
- (15) Andya, J. D.; Hsu, C. C.; Shire, S. J. Mechanisms of aggregate formation and carbohydrate excipient stabilization of lyophilized humanized monoclonal antibody formulations. *AAPS PharmSci* **2003**, *5* (2), 21–31.
- (16) Brych, S. R.; Gokarn, Y. R.; Hultgen, H.; Stevenson, R. J.; Rajan, R.; Matsumura, M. Characterization of antibody aggregation: Role of buried, unpaired cysteines in particle formation. *J. Pharm. Sci.* **2010**, *99* (2), 764–781.
- (17) Vázquez-Rey, M.; Lang, D. A. Aggregates in monoclonal antibody manufacturing processes. *Biotechnol. Bioeng.* **2011**, *108* (7), 1494–1508.
- (18) Beck, A.; Wagner-Rousset, E.; Ayoub, D.; Van Dorsselaer, A.; Sanglier-Cianféroni, S. Characterization of Therapeutic Antibodies and Related Products. *Anal. Chem.* **2013**, *85* (2), 715–736.
- (19) McSherry, T.; McSherry, J.; Ozaeta, P.; Longenecker, K.; Ramsay, C.; Fishpaugh, J.; Allen, S. Cysteinylation of a monoclonal antibody leads to its inactivation. *mAbs* **2016**, *8* (4), 718–725.
- (20) Lakbub, J. C.; Shipman, J. T.; Desaire, H. Recent mass spectrometry-based techniques and considerations for disulfide bond characterization in proteins. *Anal. Bioanal. Chem.* **2018**, *410* (10), 2467–2484.
- (21) Wu, S.-L.; Jiang, H.; Lu, Q.; Dai, S.; Hancock, W. S.; Karger, B. L. Mass Spectrometric Determination of Disulfide Linkages in Recombinant Therapeutic Proteins Using Online LC–MS with Electron-Transfer Dissociation. *Anal. Chem.* **2009**, *81* (1), 112–122.
- (22) Wu, S.-L.; Jiang, H.; Hancock, W. S.; Karger, B. L. Identification of the Unpaired Cysteine Status and Complete Mapping of the 17 Disulfides of Recombinant Tissue Plasminogen Activator Using LC–MS with Electron Transfer Dissociation/Collision Induced Dissociation. *Anal. Chem.* **2010**, *82* (12), 5296–5303.
- (23) Bagal, D.; Valliere-Douglass, J. F.; Balland, A.; Schnier, P. D. Resolving Disulfide Structural Isoforms of IgG2 Monoclonal Antibodies by Ion Mobility Mass Spectrometry. *Anal. Chem.* **2010**, *82* (16), 6751–6755.
- (24) Atmanene, C. d.; Wagner-Rousset, E.; Malissard, M.; Chol, B.; Robert, A.; Corvaia, N.; Dorsselaer, A. V.; Beck, A.; Sanglier-Cianféroni, S. Extending Mass Spectrometry Contribution to Therapeutic Monoclonal Antibody Lead Optimization: Characterization of Immune Complexes Using Noncovalent ESI-MS. *Anal. Chem.* **2009**, *81* (15), 6364–6373.
- (25) McCullough, B. J.; Kalapothakis, J.; Eastwood, H.; Kemper, P.; MacMillan, D.; Taylor, K.; Dorin, J.; Barran, P. E. Development of an Ion Mobility Quadrupole Time of Flight Mass Spectrometer. *Anal. Chem.* **2008**, *80* (16), 6336–6344.
- (26) Echterbille, J.; Quinton, L.; Gilles, N.; De Pauw, E. Ion Mobility Mass Spectrometry as a Potential Tool To Assign Disulfide Bonds Arrangements in Peptides with Multiple Disulfide Bridges. *Anal. Chem.* **2013**, *85* (9), 4405–4413.
- (27) Massonnet, P.; Upert, G.; Smargiasso, N.; Gilles, N.; Quinton, L.; De Pauw, E. Combined Use of Ion Mobility and Collision-Induced Dissociation To Investigate the Opening of Disulfide Bridges by Electron-Transfer Dissociation in Peptides Bearing Two Disulfide Bonds. *Anal. Chem.* **2015**, *87* (10), 5240–5246.
- (28) Massonnet, P.; Haler, J. R.; Upert, G.; Degueldre, M.; Morsa, D.; Smargiasso, N.; Mourier, G.; Gilles, N.; Quinton, L.; De Pauw, E. Ion Mobility-Mass Spectrometry as a Tool for the Structural Characterization of Peptides Bearing Intramolecular Disulfide Bond(s). *J. Am. Soc. Mass Spectrom.* **2016**, *27* (10), 1637–46.
- (29) Delvaux, C.; Massonnet, P.; Kune, C.; Haler, J. R. N.; Upert, G.; Mourier, G.; Gilles, N.; Quinton, L.; De Pauw, E.; Far, J. Combination of Capillary Zone Electrophoresis-Mass Spectrometry, Ion Mobility-Mass Spectrometry, and Theoretical Calculations for Cysteine Connectivity Identification in Peptides Bearing Two Intramolecular Disulfide Bonds. *Anal. Chem.* **2020**, *92* (3), 2425–2434.
- (30) Dit Fouque, K. J.; Moreno, J.; Hegemann, J. D.; Zirah, S.; Rebuffat, S.; Fernandez-Lima, F. Identification of Lasso Peptide Topologies Using Native Nanoelectrospray Ionization-Trapped Ion Mobility Spectrometry–Mass Spectrometry. *Anal. Chem.* **2018**, *90* (8), 5139–5146.
- (31) Jeanne Dit Fouque, K.; Bisram, V.; Hegemann, J. D.; Zirah, S.; Rebuffat, S.; Fernandez-Lima, F. Structural signatures of the class III lasso peptide BI-32169 and the branched-cyclic topoisomers using trapped ion mobility spectrometry-mass spectrometry and tandem mass spectrometry. *Anal. Bioanal. Chem.* **2019**, *411* (24), 6287–6296.
- (32) Schmitz, T.; Pengelley, S.; Belau, E.; Suckau, D.; Imhof, D. LC-Trapped Ion Mobility Spectrometry-TOF MS Differentiation of 2- and 3-Disulfide-Bonded Isomers of the μ -Conotoxin PIIIA. *Anal. Chem.* **2020**, *92* (16), 10920–10924.
- (33) Giles, K.; Ujma, J.; Wildgoose, J.; Pringle, S.; Richardson, K.; Langridge, D.; Green, M. A Cyclic Ion Mobility-Mass Spectrometry System. *Anal. Chem.* **2019**, *91* (13), 8564–8573.
- (34) Eldrid, C.; Ujma, J.; Kalfas, S.; Tomczyk, N.; Giles, K.; Morris, M.; Thalassinos, K. Gas Phase Stability of Protein Ions in a Cyclic Ion Mobility Spectrometry Traveling Wave Device. *Anal. Chem.* **2019**, *91* (12), 7554–7561.
- (35) Sisley, E. K.; Ujma, J.; Palmer, M.; Giles, K.; Fernandez-Lima, F. A.; Cooper, H. J. LESA Cyclic Ion Mobility Mass Spectrometry of Intact Proteins from Thin Tissue Sections. *Anal. Chem.* **2020**, *92*, 6321.
- (36) Beck, A.; Bussat, M. C.; Haeuw, J. F.; Corvaia, N.; Nguyen, T. N.; Bonnefoy, J. Y.; Zorn, N.; Van Dorsselaer, A. Synthesis and characterization of Respiratory Syncytial Virus protein G related peptides containing two disulfide bridges. *J. Pept. Res.* **2000**, *55* (1), 24–35.
- (37) Polasky, D. A.; Dixit, S. M.; Fantin, S. M.; Ruotolo, B. T. CIUSuite 2: Next-Generation Software for the Analysis of Gas-Phase Protein Unfolding Data. *Anal. Chem.* **2019**, *91* (4), 3147–3155.